

ESI for “Src kinase slows collective rotation of confined epithelial cell monolayers”

Nastassia Pricoupenko^{1*}, Flavia Marsigliesi^{1*}, Philippe Marcq²,
Carles Blanch-Mercader¹, and Isabelle Bonnet¹

¹Institut Curie, Université PSL, Sorbonne Université, CNRS
UMR168, Physics of Cells and Cancer, F-75005 Paris, France
²Physique et Mécanique des Milieux Hétérogènes, PMMH, CNRS,
ESPCI Paris, Université PSL, Sorbonne Université, Université
Paris Cité, F-75005, Paris, France

*Equal contribution

Contents

1	Theoretical model	2
2	Additional expression of steady-state mechanical fields	4
3	References	4
4	Supplementary Figures	6
5	Supporting Movies	16

1 Theoretical model

In this section, we detail the theoretical framework used to describe monolayers of cells [1]. For more details on the active gel theory we refer to Refs [2, 3, 4].

The cell monolayers are characterised by the coarse-grained cell velocity field \mathbf{v} and the coarse-grained cell polarity field \mathbf{p} . As explained in the main text, we consider the system incompressible and as a consequence the cell number density n is constant. Because source and sinks of mass, such as cell division or apoptosis, are ignored, the incompressibility condition reduces to $\nabla \cdot \mathbf{v} = 0$. In the absence of inertial effects, the momentum conservation equation reduces to the force balance equation

$$\partial_\beta \sigma_{\alpha\beta} = T_\alpha \quad (1)$$

The gradients of total 2d stresses σ are balanced by the traction forces \mathbf{T} that arise from interaction forces between cells and the underlying substrate. For the traction forces, we consider the special case

$$T_\alpha = \xi v_\alpha - T_0 p_\alpha \quad (2)$$

that includes two contributions that is a viscous friction proportional to the velocity field \mathbf{v} , with a friction coefficient ξ , and active traction forces proportional to the polarity field \mathbf{p} , with an amplitude T_0 . For a more general discussion of the traction forces, we refer to [5].

To build the constitutive relations of the system, we follow the standard approach of non-equilibrium thermodynamics [6]. It consists of first identifying pairs of conjugated thermodynamic forces and fluxes by inspecting the time derivative of the free energy. In a second step, the fluxes are expressed to linear order in terms of the forces, where the coupling coefficients obey the Onsager relations.

Here, we choose the following quantities as thermodynamic forces [2, 3, 4]: the symmetric part of the velocity gradient tensor with components $v_{\alpha\beta} = (\partial_\alpha v_\beta + \partial_\beta v_\alpha)/2$, the field $\mathbf{h} = -\delta\mathcal{F}/\delta\mathbf{p}$, where \mathcal{F} is the equilibrium free energy, and the chemical potential difference $\Delta\mu$ of the fuel consumption reaction, typically ATP hydrolysis in cells. The corresponding thermodynamic fluxes are given by the deviatoric stress tensor σ^d , the co-rotational convective derivative of the polarization field $D\mathbf{p}/Dt$, and the rate r of ATP-hydrolysis. The deviatoric stress tensor is defined as $\sigma^d = \sigma - \sigma^e$ the difference between the total stress tensor σ and the Ericksen stress σ^e . The co-rotational convective derivative of the polarization field is given by

$$\frac{Dp_\alpha}{Dt} = \partial_t p_\alpha + v_\beta \partial_\beta p_\alpha + \omega_{\alpha\beta} p_\beta. \quad (3)$$

where $\omega_{\alpha\beta} = (\partial_\alpha v_\beta - \partial_\beta v_\alpha)/2$ is the antisymmetric part of the velocity gradient tensor. As we assume $\Delta\mu$ to be constant, we do not consider r any further.

The deviatoric stress and the co-rotational convective derivative of the polarization field are

$$\begin{aligned} \sigma_{\alpha\beta}^d &= 2\eta v_{\alpha\beta} + \frac{\nu}{2} (p_\alpha h_\beta + p_\beta h_\alpha - p_\gamma h_\gamma \delta_{\alpha\beta}) \\ &\quad - \zeta \Delta\mu \left(p_\alpha p_\beta - \frac{1}{2} p_\gamma p_\gamma \delta_{\alpha\beta} \right) + \frac{1}{2} \tau \Delta\mu (p_\alpha p_\beta^\perp + p_\beta p_\alpha^\perp) \end{aligned} \quad (4)$$

$$\frac{Dp_\alpha}{Dt} = \frac{h_\alpha}{\gamma} - \nu v_{\alpha\beta} p_\beta \quad (5)$$

where we used the incompressibility condition $v_{\gamma\gamma} = 0$ to simplify these expressions, and redefine the pressure field P such that $\sigma_{\gamma\gamma}^d = 0$. In Eq. (4), the first term accounts for viscous stresses, where the coefficient η is the shear viscosity. The second term couples the mechanical stresses to the field \mathbf{h} . The remaining terms couple the mechanical stress to ATP-hydrolysis. The term proportional to the coefficient ζ denotes the achiral components of the active stresses, whereas the term proportional to the coefficient τ denotes the chiral components of the active stresses [7]. The field \mathbf{p}^\perp corresponds to the perpendicular vector to the polarity field. In Eq. (5), the first term captures relaxation of the polarization field with γ being a rotational viscosity. The second term describe the re-orientation of the polarity field to shear flows. The coefficient ν is the so-called shear flow-alignment parameter. Note that, in this equation, we have omitted an active term, that is a coupling to $\Delta\mu$. One of these terms would be of the form $\lambda_1 \Delta\mu p_\alpha$ and it amounts to a renormalization of parameters [2, 3]. Another of such terms would be of the form $\lambda_2 \Delta\mu p_\alpha^\perp$, which describes the active spinning of the polarity field, and it necessitates a substrate to exists.

Explicit expressions for the Ericksen stress σ^e and the field \mathbf{h} are obtained by fixing the equilibrium free energy \mathcal{F} of the system. We choose:

$$\mathcal{F} = \int_{\mathcal{A}} \left\{ \frac{\chi}{2} p_\alpha^2 + \frac{\kappa}{2} (\partial_\alpha p_\beta)^2 \right\} da. \quad (6)$$

The two terms capture the elastic energy associated with distortions of the polarization field similar to the free energy used for liquid crystals [8]. Here, we consider $\chi > 0$ meaning that the preferred bulk equilibrium state is disordered. The energy cost associated with gradients of the polarization field is accounted for by the second term. It is equal to the Frank energy in the one-constant approximation with modulus κ .

Based on the free energy (6), the expression for the Ericksen stress is

$$\sigma_{\alpha\beta}^e = -P \delta_{\alpha\beta} - \kappa \left(\partial_\alpha p_\gamma \partial_\beta p_\gamma - \frac{1}{2} \partial_\rho p_\gamma \partial_\rho p_\gamma \delta_{\alpha\beta} \right) + \frac{1}{2} (p_\alpha h_\beta - p_\beta h_\alpha) \quad (7)$$

and of the molecular field \mathbf{h} is

$$h_\alpha = -\frac{\delta\mathcal{F}}{\delta p_\alpha} = -\chi p_\alpha + \kappa \partial_{\gamma\gamma} p_\alpha. \quad (8)$$

To obtain the continuum equations in the main text, we make the following simplifying approximations. In Eq. (5), we approximate $Dp_\alpha/Dt \approx 0$ and ignore the effect of the shear-flow alignment by setting $\nu = 0$. Besides, the angle between the polarity field and the radial direction ψ is considered to be uniform. In Eq. (4), the stress that arises from couplings with the field \mathbf{h} and both active stresses are ignored by setting $\nu = \zeta = \tau = 0$. In addition, the off-diagonal components of the Ericksen stress are ignored. The importance of some of these approximations in describing cell monolayers is discussed in appendix A.

2 Additional expression of steady-state mechanical fields

Below, we provide the analytical solutions of additional mechanical fields

$$T_r(r) = \frac{-T_o \cos(\psi) I_1(r/L_c)}{I_1(R/L_c)} \quad (9)$$

$$T_\theta(r) = \frac{T_o \sin(\psi) L_\eta}{(L_c^2 - L_\eta^2)} \frac{L_\eta I_1(r/L_c) I_2(R/L_\eta) - L_c I_1(r/L_\eta) I_2(R/L_c)}{I_1(R/L_c) I_2(R/L_\eta)} \quad (10)$$

$$\sigma_{r\theta}(r) = \frac{T_o \sin(\psi) L_\eta^2 L_c}{(L_c^2 - L_\eta^2)} \frac{I_2(r/L_c) I_2(R/L_\eta) - I_2(r/L_\eta) I_2(R/L_c)}{I_1(R/L_c) I_2(R/L_\eta)} \quad (11)$$

$$\sigma_{\theta\theta}(r) = -P(r) = T_o L_c \cos(\psi) \frac{I_0(\frac{R}{L_c}) - I_0(\frac{r}{L_c})}{I_1(\frac{R}{L_c})} \quad (12)$$

which complement Eqs. (8-10) in the main text. The function $I_n(x)$ is a modified Bessel function of the first kind of order n . The parameter R corresponds to the radius of the circular confinement, and $L_c = \sqrt{\kappa/\chi}$ and $L_\eta = \sqrt{\eta/\xi}$ are two characteristic lengthscales of the system. The other parameters are defined above and for more details, see also the main text.

3 References

- [1] Carles Blanch-Mercader, Pau Guillamat, Aurélien Roux, and Karsten Kruse. Integer topological defects of cell monolayers: Mechanics and flows. *Physical Review E*, 103:012405, 2021.
- [2] Karsten Kruse, Jean-Francois Joanny, Frank Jülicher, Jacques Prost, and Ken Sekimoto. Generic theory of active polar gels: a paradigm for cytoskeletal dynamics. *The European Physical Journal E*, 16:5–16, 2005.
- [3] Jean-François Joanny, Frank Jülicher, Karsten Kruse, and Jacques Prost. Hydrodynamic theory for multi-component active polar gels. *New Journal of Physics*, 9(11):422, 2007.
- [4] Frank Jülicher, Stephan W Grill, and Guillaume Salbreux. Hydrodynamic theory of active matter. *Reports on Progress in Physics*, 81(7):076601, 2018.

- [5] Frank Jülicher and Jacques Prost. Generic theory of colloidal transport. *The European Physical Journal E*, 29:27–36, 2009.
- [6] Sybren Ruurds De Groot and Peter Mazur. *Non-equilibrium thermodynamics*. Courier Corporation, 2013.
- [7] Ludwig A Hoffmann, Koen Schakenraad, Roeland MH Merks, and Luca Giomi. Chiral stresses in nematic cell monolayers. *Soft matter*, 16(3):764–774, 2020.
- [8] Pierre-Gilles De Gennes and Jacques Prost. *The physics of liquid crystals*. Oxford university press, 1993.

4 Supplementary Figures

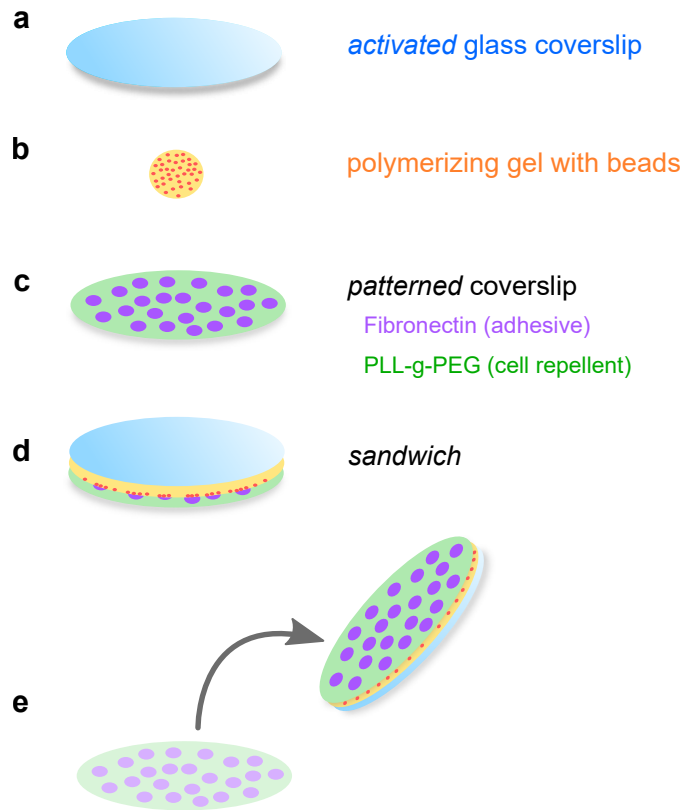


Fig. S1: Preparation of patterned gels for Traction Force Microscopy. **a** A silanized glass coverslip is *activated* with glutaraldehyde. **b** Mix of acrylamide and bis-acrylamide necessary to obtain specific stiffness, containing fluorescent beads. **c** Circular islands of fibronectin are micropatterned on PLL-g-PEG-coated coverslip using chrome mask and deep UV exposure. **d** The drop of polymerizing gel is *sandwiched* between the two coverslips. **e** Once the glass coverslips are detached from each other, the *activated* coverslip will be covered with polyacrylamide gel coated with a layer of cell repellent PLL-g-peg and cell adhesive fibronectin patterns. See Methods for details.

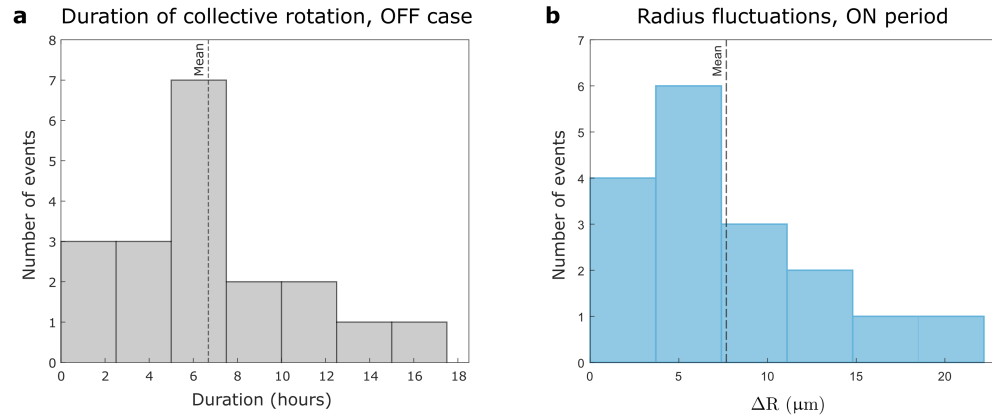


Fig. S2: **a-Duration of collective-rotation events for non-activated MDCK optoSrc cells.** Monolayers of MDCK optoSrc cells were confined in 100 μm -radius disk and kept indefinitely in the dark. The duration of the collective rotation was measured manually, we found an average rotation time of 7 ± 4 hours (standard deviation, $N = 19$ colonies) of uninterrupted rotation. **b-Fluctuations in radius ΔR during Src activation.** ΔR was estimated by considering the time point during the ON period (often, but not necessarily, the last) for which the colony area A is maximal: $\Delta R = \frac{R\Delta A}{2A}$ with $\Delta A = A_{\text{max}} - A$ where $A = \pi R^2$ being the area of the circular pattern ($N = 17$ colonies).

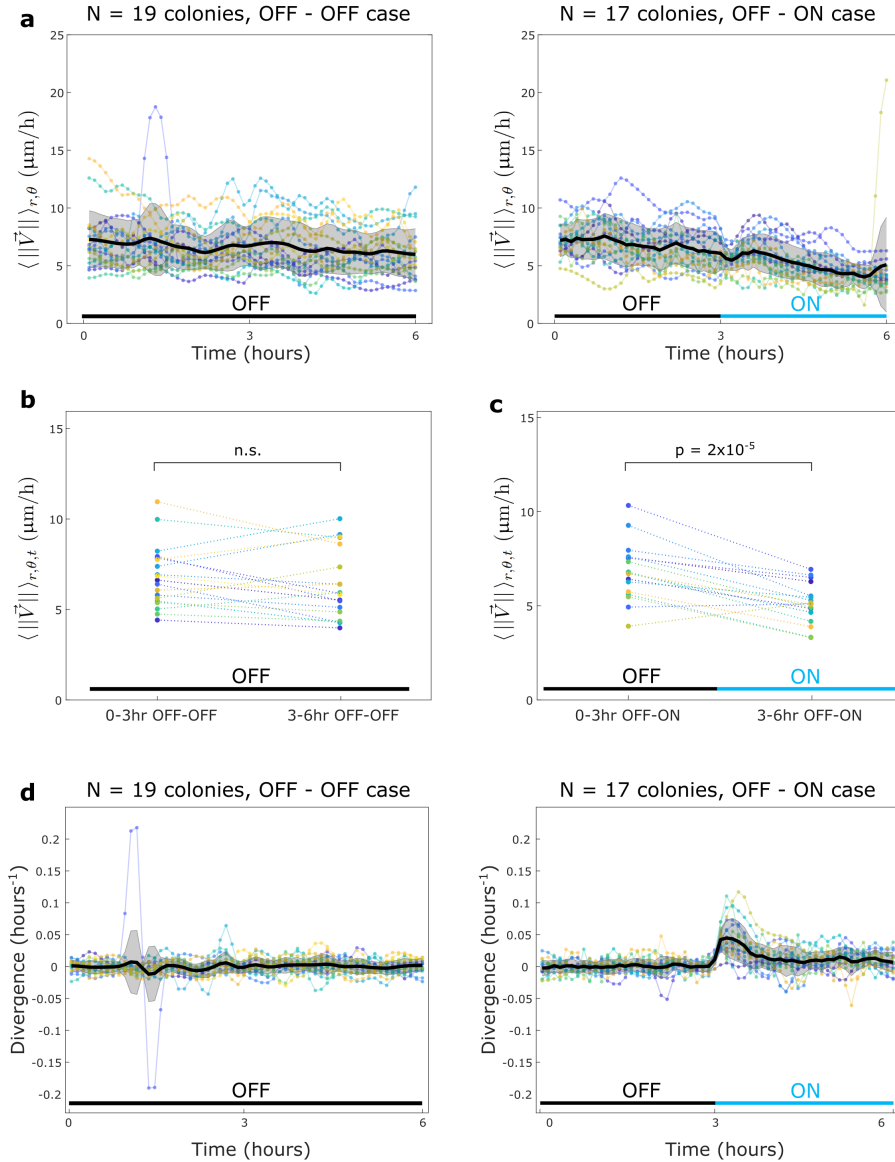


Fig. S3: Src activation reduces velocity magnitude. **a** Time evolution of the space-averaged speed $\left(\langle \|\vec{V}\| \rangle_{r,\theta}\right)$ for all colonies (one color = one colony) for control experiments (left) and Src activation experiments (right). **b-c** For each colony, we time-averaged $\langle \|\vec{V}\| \rangle_{r,\theta}$ over the two periods (first 3 and last 3 hrs) for the control case (b) and during Src activation (c). T-tests on paired data were used after verifying normality (Shapiro-Wilk test), n.s. stands for non significant when $p > 0.05$. **d** Spatially-averaged divergence of the velocity field during OFF-OFF (left) and OFF-ON experiments (right). In panels a and d, black lines represent population averages and shaded areas indicate one standard deviation (one color = one colony).

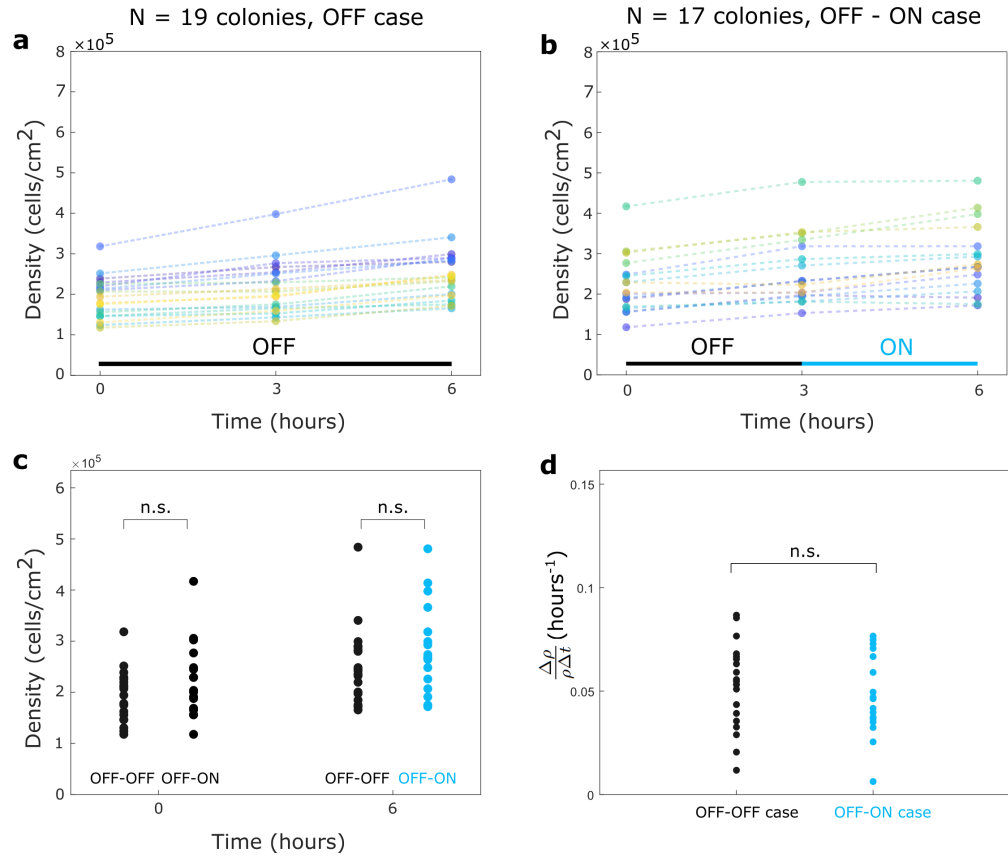


Fig. S4: Time evolution of cell density. **a-b** Cell density of all colonies (one color = one colony) at three different time-points (0, 3 hrs, 6 hrs) for control experiments (a) and during Src activation (OFF-ON case, b). **c** Comparison of initial ($t = 0$, left) and final ($t = 6$ hrs, right) cell density between the two types of experiments. **d** Density variation rate over the course of experiment ($\Delta t = 6$ hrs) for control experiments and during Src activation. Mann Whitney-U tests indicate no significant difference (n.s. for $p > 0.05$).

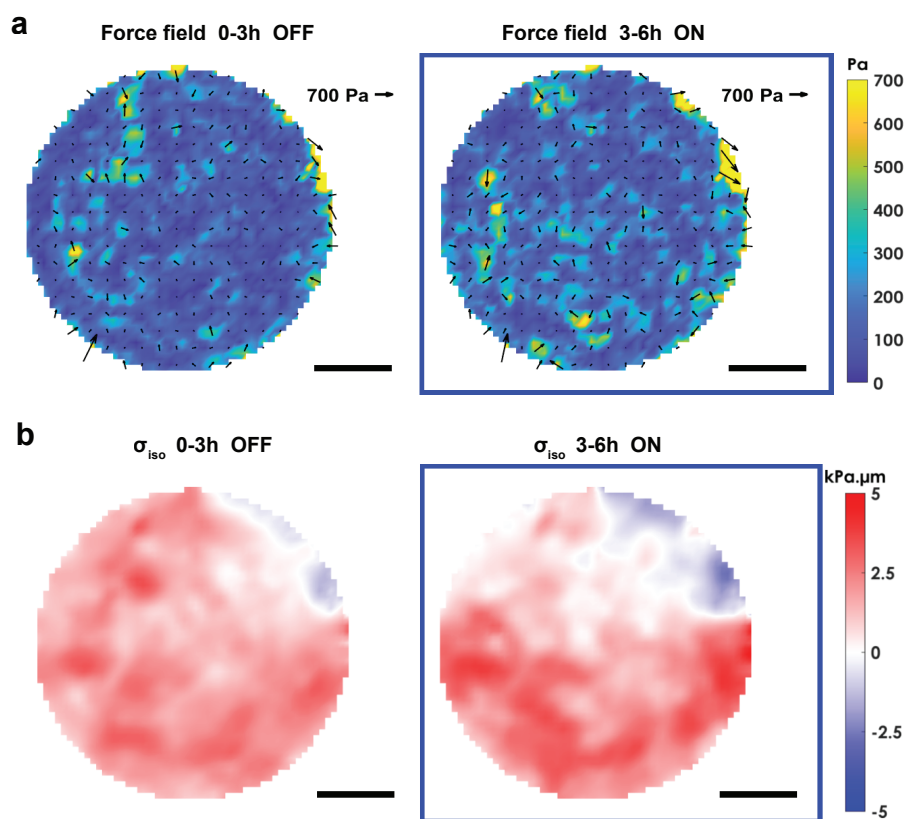


Fig. S5: **Traction force field and isotropic stress during OFF/ON experiment.** **a** Plot of the time-averaged traction forces magnitude superimposed with traction forces vector plot obtained by TFM for the first 3 hours (left, OFF) and for the last 3 hours (right, ON, Src is activated). For visibility, only one arrow out of three is drawn. Traction forces are surfacic and thus expressed in Pa. **b** Plot of the time-averaged tension $\sigma_{iso} = (\sigma_{rr} + \sigma_{\theta\theta})/2$ measured by BISM over the first 3 hours (left, OFF) and over the last 3 hours (ON, right, Src is activated). 2d stresses are expressed in kPa· μm . Same colony as in Fig. 2, Movie 2. Scale bars: 50 μm .

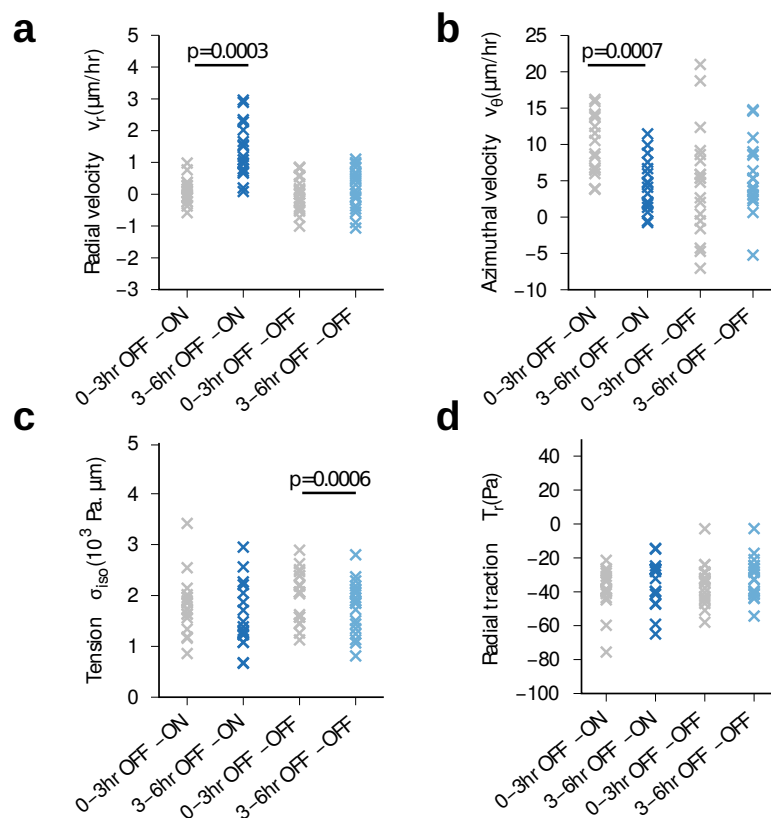


Fig. S6: **Spatially-averaged physical fields in the OFF-ON and OFF-OFF experiments.** **a** Radial velocity component. **b** Azimuthal velocity component. **c** Isotropic stress $\sigma_{iso} = (\sigma_{rr} + \sigma_{\theta\theta})/2$. **d** Radial tractions. All physical variables were averaged on a circle of radius R , the confinement radius. Normality was checked (Shapiro-Wilk test), and T-tests on paired data were performed between the cases 0-3 hrs OFF-ON and 3-6 hrs OFF-ON and the cases 0-3 hrs OFF-OFF and 3-6 hrs OFF-OFF. Non significant p-values ($p > 0.01$) are not shown.

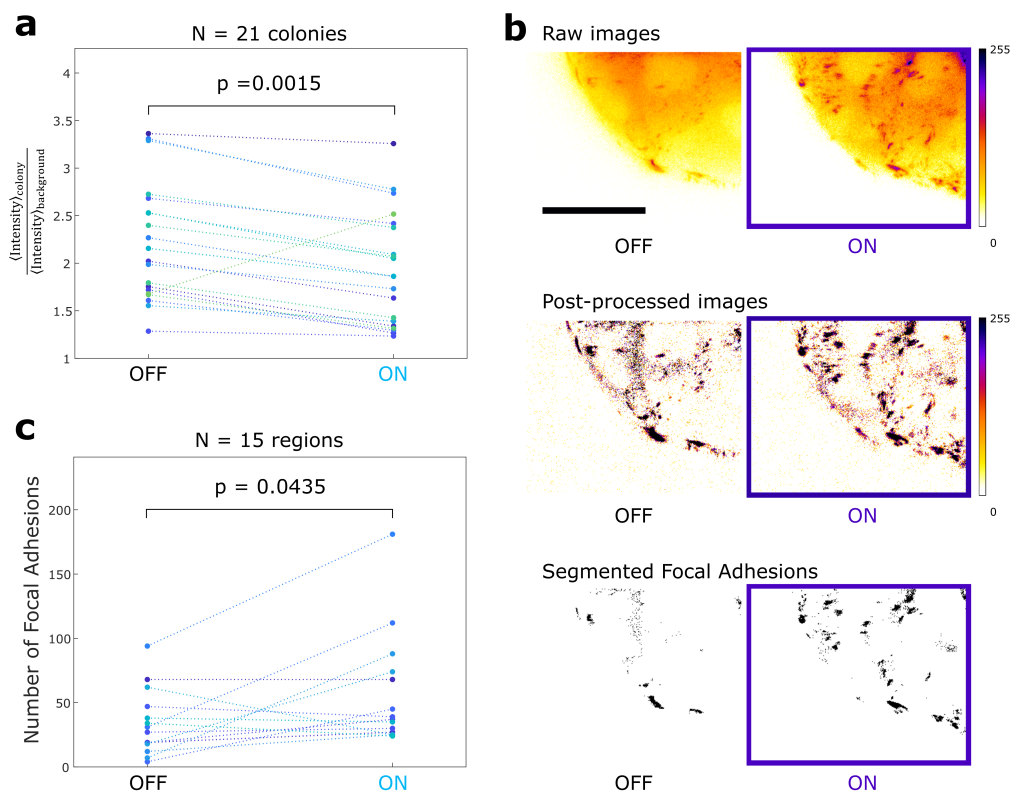


Fig. S7: Quantitative analysis of vinculin distribution. **a** Mean intensity of vinculin-iRFP between OFF and ON for all the colonies imaged ($N = 21$). The mean intensity inside the circular pattern (colony) was normalized by the mean intensity in a region outside the pattern (background). The tendency to decrease could be associated with the bleaching of the iRFP. **b** An example of cropped region used in our pipeline to segment focal adhesions (left: cells kept in the dark, right: same region after 1 hr of Src activation). Top: raw images, middle: images after processing, bottom: segmented focal adhesions. Scale bar: 25 μm . **c** Comparison of the number of focal adhesions between OFF and ON for $N = 15$ analyzed regions. Wilcoxon signed-rank tests were used to check the significance, as the distributions were not normal. See Methods for details about the image analysis steps.

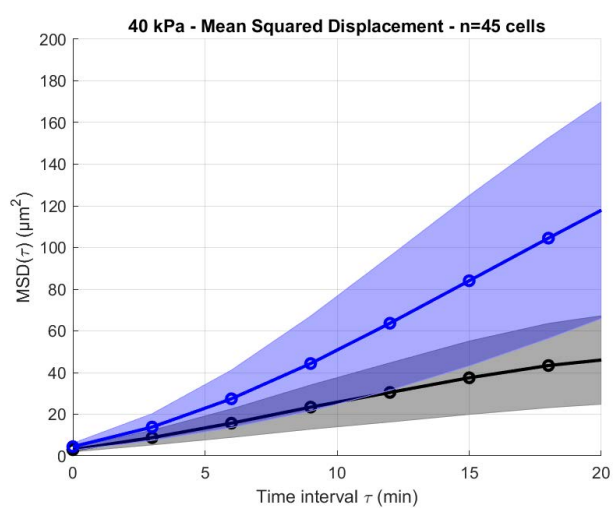


Fig. S8: Mean Square Displacement (MSD) for isolated MDCK **optoSrc** cells kept in the dark or illuminated with blue light. $N = 45$ isolated cells were subjected to a sequence of 1 hr in the dark then 1 hr under blue light, and their center of mass was tracked over time. This gives 45 one-hour tracks for each period. Ensemble-average MSD derived from all tracks OFF (black) and all tracks ON (blue) are shown for the first 20 min for statistical significance. The error bars represent the 95% confidence interval for the mean.

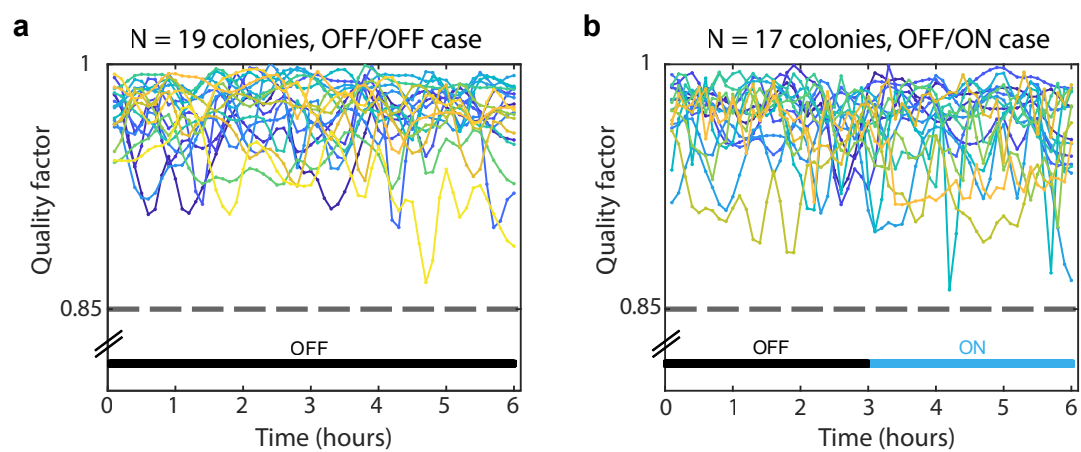


Fig. S9: **Quality factor of traction forces reconstruction.** The quality factor is plotted as a function of time for all colonies kept in the dark (left, $N = 19$ colonies), or subjected to the transient Src activation (right, $N = 17$ colonies). Each colony is represented by a color. The dashed horizontal represents the threshold we have set to estimate that the force reconstruction is acceptable.

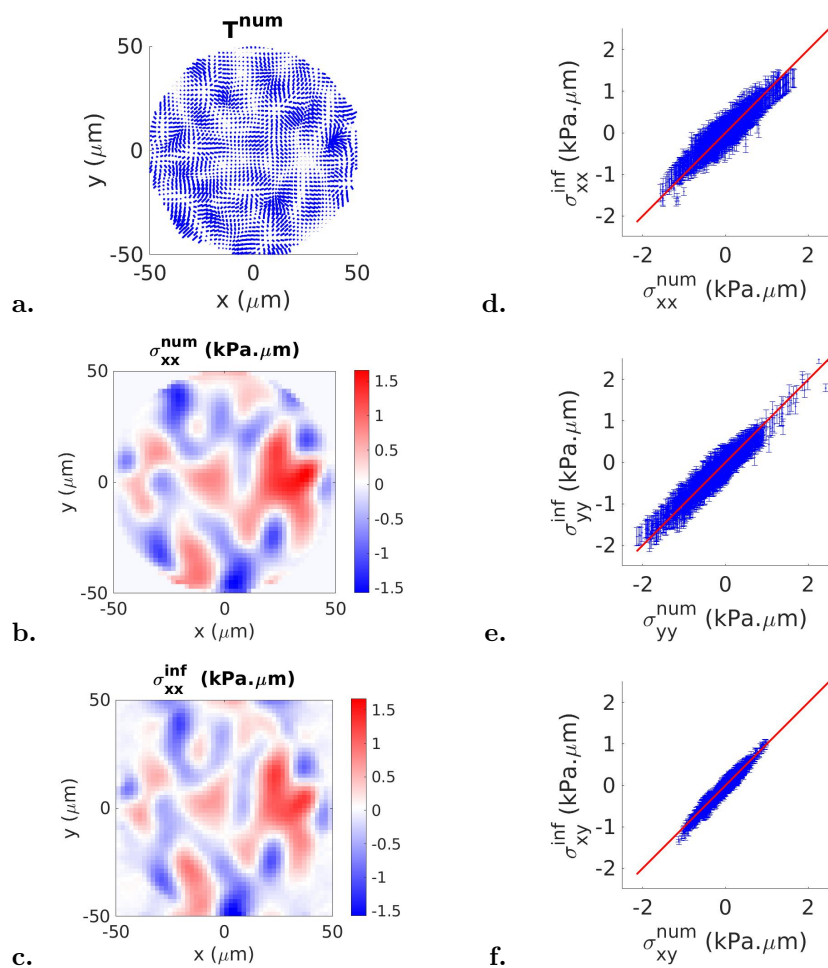
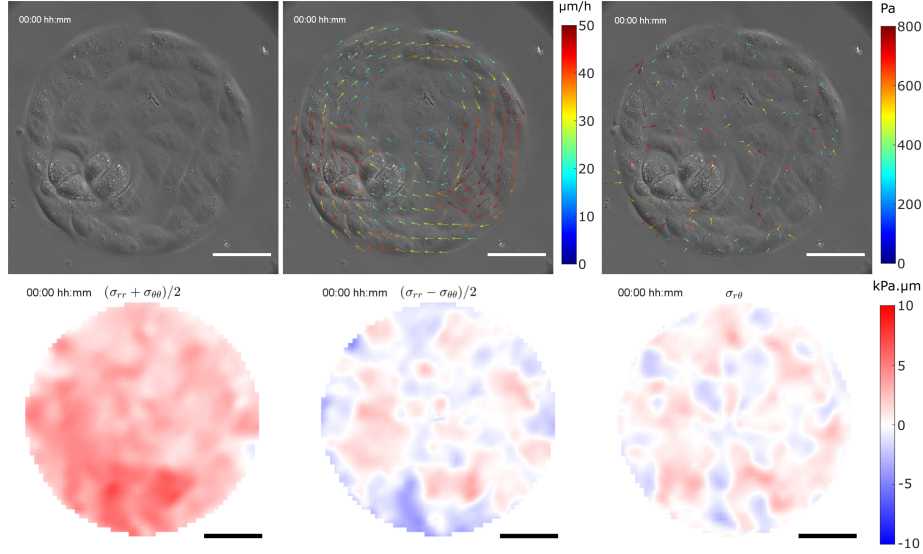


Fig. S10: **Bayesian inversion stress microscopy.** **a.** Simulated traction force field \vec{T}^{num} . **b.** Simulated stress field x component σ_{xx}^{num} . **c.** Inferred stress field x component σ_{xx}^{inf} . Note the high degree of similarity between images (b) and (c). **d-f** Plots of the inferred stress *vs.* the simulated stress for each component. Error bars correspond to one standard deviation, and the red line is the bisector $y = x$. All 2d stresses are given in $\text{kPa}\cdot\mu\text{m}$

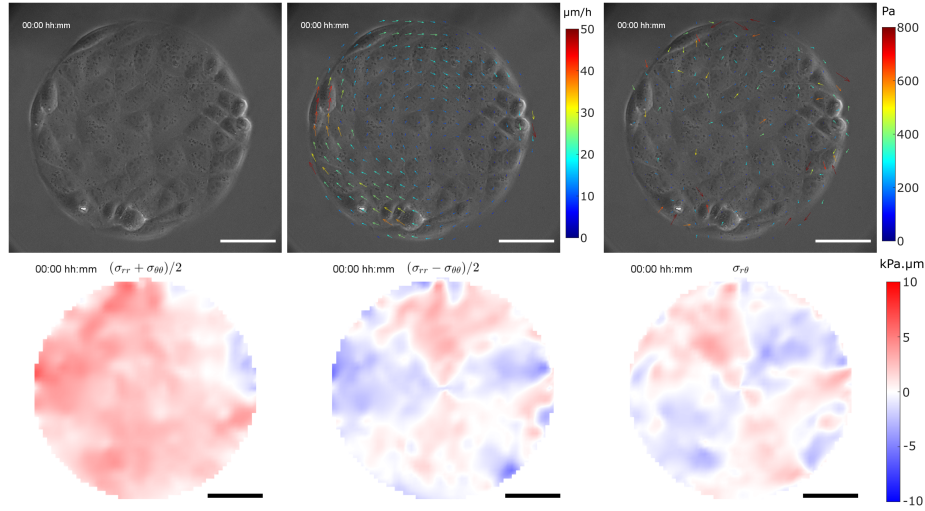
5 Supporting Movies



Mechanical state of confined MDCK optoSrc cells in the dark (first frame of Movie 1). A typical example of a 6-hour movie of a monolayer of MDCK optoSrc cells, kept in the dark, confined in a 100- μm radius circle, on a polyacrylamide gel of ~ 40 kPa, displaying collective rotation. In that case, there is no blue stimulation. 1 image every 15 min. Scale bar: 50 μm . Same colony as in Fig. B1.

Top-left: phase-contrast images. **Top-middle:** velocity field obtained by PIV and superimposed on the phase-contrast images. Color codes for speed, expressed in $\mu\text{m}/\text{h}$. For PIV computation, we used a window size of 128 pixels with 0.5 overlap. Arrows are then interpolated on the TFM grid, and only one of every three is drawn. **Top-right:** traction forces field obtained by TFM and superimposed on the phase-contrast images. Color codes for traction amplitude, in Pascal. The inter-spacing is 16 pixels, but only one arrow of every two is drawn.

Bottom: Stress components as estimated by BISM. Stresses are given in $\text{kPa}\cdot\mu\text{m}$, with the same color code in all panels. **Left:** tension $(\sigma_{rr} + \sigma_{\theta\theta})/2$. **Central:** deviatoric component $(\sigma_{rr} - \sigma_{\theta\theta})/2$. **Right:** shear stress $\sigma_{r\theta}$.



Mechanical state of confined MDCK optoSrc cells during OFF/ON experiment (first frame of Movie 2). A typical example of a 6-hour movie of a monolayer of MDCK optoSrc cells, submitted to the OFF/ON sequence, confined in a 100- μm radius circle, on a polyacrylamide gel of ~ 40 kPa. During the first 3 hours, the monolayer displays a collective rotation. From $t = 3$ h (blue frame), the whole field of view is illuminated with a blue-light pulse every 3 min, the collective rotation is disrupted and the optoSrc cells go outside the pattern. 1 image every 15 min. Scale bar: 50 μm . Same colony as in Fig. 2 and Fig. S5.

Top-left: phase-contrast images. **Top-middle:** velocity field obtained by PIV and superimposed on the phase-contrast images. Color codes for speed, expressed in $\mu\text{m}/\text{h}$. For PIV computation, we used a window size of 128 pixels with 0.5 overlap. Arrows are then interpolated on the TFM grid, and only one of every three is drawn. **Top-right:** traction forces field obtained by TFM and superimposed on the phase-contrast images. Color codes for traction amplitude, in Pascal. The inter-spacing is 16 pixels, but only one arrow of every three is drawn.

Bottom: Stress components as estimated by BISM. Stresses are given in $\text{kPa}\cdot\mu\text{m}$, with the same color code in all panels. **Left:** tension $(\sigma_{rr} + \sigma_{\theta\theta})/2$. **Central:** deviatoric component $(\sigma_{rr} - \sigma_{\theta\theta})/2$. **Right:** shear stress $\sigma_{r\theta}$.